ELSEVIER

Journal of Power Sources 102 (2001) 167–171

JOURNAL OF POWER SOURCES

www.elsevier.com/locate/jpowsour

Electrochemical and structural properties of radio frequency sputtered cobalt oxide electrodes for thin-film supercapacitors

Han-Ki Kim[a,c], Tae-Yeon Seong[c], Jae-Hong Lim[a], Won Ii Cho[b], Young Soo Yoon[a,*]

[a]*Thin-Film Technology Research Centre, Korea Institute of Science and Technology (KIST), P.O. Box 131, Choengryang, Seoul 130-650, South Korea*
[b]*Battery and Fuel Cell Centre, Korea Institute of Science and Technology (KIST), P.O. box 131, Choengryang, Seoul 130-650, South Korea*
[c]*Department of Materials Science and Engineering, Kwangju Institute of Science and Technology (K-JIST), Kwangju 500-712, South Korea*

Received 30 March 2001; accepted 6 April 2001

Abstract

The electrochemical and structural properties of cobalt oxide films which are deposited at different sputtering gas-ratios of $O_2/(Ar + O_2)$ are investigated. In order to examine the electrochemical properties of the as-deposited films, all solid-state thin-film supercapacitors (TFSCs) are fabricated. There consist of Co_3O_4 electrodes and an amorphous LiPON thin-film electrolyte. It is shown that the capacitance behaviour of the Co_3O_4/LiPON/Co_3O_4 TFSCs is similar to bulk-type supercapacitor behaviour. It is further shown that the electrochemical behaviour of the TFSCs is dependent on the sputtering gas-ratios. The gas-ratio dependence of the capacitance of the oxide electrode films is discussed based on X-ray diffraction (XRD) and electrical results for the Co_3O_4 films. © 2001 Published by Elsevier Science B.V.

Keywords: Thin-film; Supercapacitor; Co_3O_4; LiPON electrolyte; Gas-ratio; Capacitance

1. Introduction

Oxide film-based thin-film supercapacitors (TFSCs) have been the subject of considerable attention as energy-storage systems, particularly for applications which involve a micro-power sources for microelectronic mechanical systems (MEMS) and for back-up power sources for computer memory chips. Particularly, hybrid systems consisting of thin-film batteries (TFB) and TFSCs have been investigated [1–5]. In such hybrid systems, the TFSC can provide peak power during acceleration, and the TFB can then be optimised primarily for higher energy density.

Many transition metal oxides, such as RuO_x, NiO_x and IrO_x, have been shown to serve as excellent electrode materials for supercapacitors with their charge-storage mechanisms based on pseudocapacitance [6–8]. In particular, amorphous RuO_2 has been found to be an excellent electrode, which exhibits a high specific capacitance (720 F g^{-1}) [7]. Recently, our group reported all solid-state TFSCs which consist of an amorphous RuO_2 electrode and a LiPON electrolyte [9–11]. Due to the high cost, however, Ru is less attractive for commercial applications. Therefore, it is necessary to develop less-expensive electrode materials for TFSCs. Conway [6] investigating several electrode materials for supercapacitors, reported that Co_3O_4 and CoO_2 are promising electrode materials for supercapacitors due to their intercalative pseudocapacitance properties. The Co_3O_4 electrode has been found to have good efficiency and long-term performance. Moreover, the good corrosion stability of the Co_3O_4 electrode and its low cost are attractive properties for the fabrication of highly stable TFSCs [12,13]. Liu et al. [14] investigating the redox behaviour and charge-storage mechanism of thick cobalt oxide films, also showed that cobalt oxide films exhibit pseudocapacitance behaviour during about 2800 cycles over the potential range of −2 (or +0.1) to −1.56 V at a sweep rate of 20 mV s^{-1}.

Although the usefulness of lithium cobalt oxide ($LiCoO_2$) in TFB has long been recognised [15], the application of the cobalt-based oxide film as an electrode material for TFSCs has not been extensively studied. To develop cobalt oxide-based electrodes for TFSCs, it is necessary to investigate the electrochemical and structural properties of cobalt oxide and to obtain an understanding of the charge-storage mechanism. The authors' research group has suggested the possibility of a TFSC using a RuO_2 electrode, but the oxygen partial flow ratio effects, which mainly influence the oxide thin-film properties, have not been explained exactly. To

* Corresponding author. Tel.: +82-2-958-5558; fax: +82-2-958-6851.
E-mail address: ysyoon@kist.re.kr (Y. Soo Yoon).

0378-7753/01/$ – see front matter © 2001 Published by Elsevier Science B.V.
PII: S0378-7753(01)00864-3

obtain a high quality, oxide thin-film, it is also imperative to determine the exact growth mechanism of the oxide films with varying oxygen flow ratio.

In this work, we report studies on all solid-state TFSCs based on Co_3O_4 thin-film electrodes and a LiPON thin-film electrolyte. It is shown that the capacitance of the TFSCs depends on the gas flow ratios $[O_2/(Ar + O_2)]$ which are used to grow the Co_3O_4 electrodes. Glancing angle XRD (GXRD) and electrical measurements show that the microstructures and carrier mobility of the Co_3O_4 electrodes depend on the gas flow ratio. Based on our previous results in developing RuO_2 electrodes for TFSC [9–11], the present work represents our continuing effort in the research for more commercial and surface stable electrodes for fabrication of an all-solid-state SFSC.

2. Experimental

The Co_3O_4 electrode films were grown on Pt/Ti/Si substrates by means of a specially designed dc reactive sputtering system using a 4 in. Co metal target (99.99% Super Conductor Material Inc.) at room temperature. The Pt films grown on the Ti adhesive layers act as current-collectors to diminish the potential drop between the electrode and the collector. Prior to the deposition of the lower layer of Co_3O_4 electrode film, the Co metal target was pre-sputtered using an Ar^+ plasma for 15 min to remove any contamination layer on the target. The lower Co_3O_4 electrode film (300 nm thick) was deposited on the Pt current-collector at a dc power of 100 W with oxygen gas flow ratios $[O_2/(Ar + O_2)]$ of 0.1, 0.2 and 0.3. The LiPON electrolyte film (l.3 μm thick) was then deposited by radio frequency (rf) reactive sputtering using a 4 in. Li_3PO_4 target. The Li_3PO_4 target was sputtered at an rf power of 300 W in pure N_2 to grow a LiPON ($Li_{2.94}PO_{2.37}L_{0.75}$) film at a flow of 50 sccm. After deposition of the LiPON film, the upper Co_3O_4 film was deposited using the same growth conditions as those for the underlying electrode film. A schematic of a Co_3O_4/LiPON/Co_3O_4 structured TFSC is shown in Fig. 1.

Charge–discharge measurements were performed with in a WBC 3000 (Wonatech) cycler. The constant current density was 50 μA cm^{-2} and the cut-off voltage was in the range 0–2 V. The microstructure of the lower Co_3O_4 film was characterised by GXRD (Philips XPERT-MPD with Cu Kα radiation). The surface morphology of the Co_3O_4 electrode film was assessed by means of scanning electron microscopy (SEM; HITACHI S-4100). The surface morphology of the LiPON electrolyte was also examined using atomic force microscopy (AFM; PSIA). The electrical properties of the Co_3O_4 electrode film was measured by a Hall automatic measuring system (Bio-Rad Co., UK) using Van der Pauw geometry.

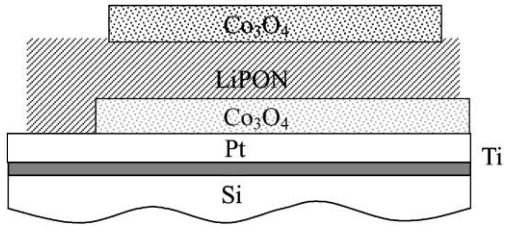

Fig. 1. Schematic diagram of Co_3O_4 electrode-based TFSC.

3. Results and discussion

The charge–discharge behaviour of the Co_3O_4/LiPON/Co_3O_4 TFSCs was examined at a current of 50 μA cm^{-2} between 0 and 2 V. The capacitance of the TFSCs as a function of cycle number is shown in Fig. 2. It is worth noting that the capacitance is improved with increasing oxygen gas flow ratio. Measurements show that the capacitance per volume of the TFSC after one cycle is 5×10^{-3}, 8.2×10^{-3}, and 2.5×10^{-2} F cm^{-2} μm for a flow ratio of 0.1, 0.2 and 0.3, respectively. It is further found that the capacitance of all the TFSCs is gradually degraded with increasing cycle number. After 400 cycles, the charge–discharge efficiency has fallen by more than 60% with respect to that on the first cycle.

Plots of voltage versus time for TFSCs containing Co_3O_4 electrodes that are grown at different oxygen flow ratios of 0.1 and 0.3, respectively, are presented in Fig. 3. The charge–discharge behaviour of both samples is similar to that of a bulk-type supercapacitor [6]. In addition, the TFSC containing the Co_3O_4 electrode grown at an oxygen flow ratio of 0.3 exhibits a longer discharge time than the sample grown at a flow of 0.1, which consistent with Fig. 2. The current–resistance (IR) drop of the TFSC is very large, however, compared with that of the typical bulk-type supercapacitors, which contain liquid-state electrolyte. The larger drop might be associated with the low ion conductivity of LiPON [10]. In other words, the ion conductivity (1.02×10^{-6} S^{-1} cm) of the solid-state LiPON electrolyte is lower than that of the liquid-state electrolyte.

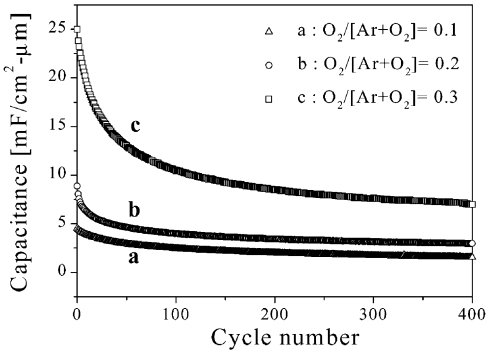

Fig. 2. Charge–discharge capacitance of Co_3O_4/LiPON/Co_3O_4 TFSC as function of cycle number. It is noted that increase in oxygen flow ratio leads to improvement of the capacitance of TFSC.

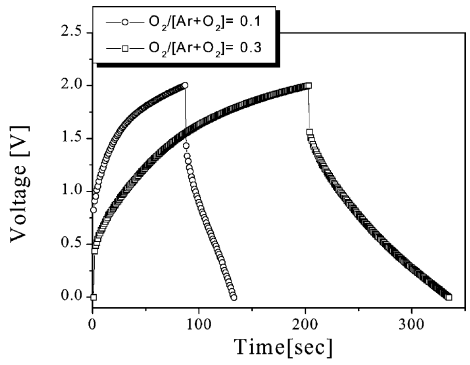

Fig. 3. Plots of voltage vs. time for TFSCs containing Co_3O_4 electrodes that are grown at a different flow ratios of 0.1 and 0.3, respectively. Charge–discharge behaviour is similar to that of bulk-type supercapacitor.

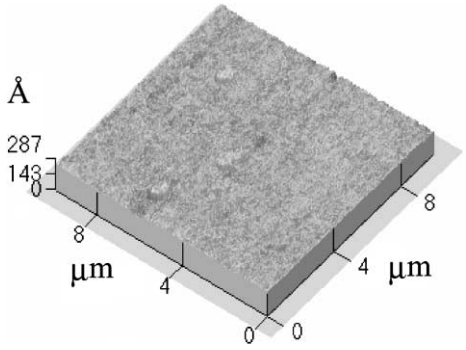

Fig. 5. AFM image of LiPON electrolyte film grown on lower Co_3O_4 film at flow ratio of 0.3.

The carrier mobility and concentration of the as-deposited Co_3O_4 electrode films as a function of the oxygen gas flow ratio are given in Fig. 4. As the flow ratio increases, the carrier mobility is increased, while the carrier concentration is decreased. Although the exact mechanism for this behaviour is not clear at present, it might be explained in terms of the incorporation of excess oxygen atoms. For oxide films grown at low oxygen gas-ratios ($\leq$0.2), there may be numerous oxygen vacancies in the oxides. Oxygen vacancies were reported to act as donors in some oxides, such as ZnO [16,17]. Thus, if the oxygen vacancies in Co_3O_4 could act as carriers, the growth at low flow ratios would result in high carrier concentrations and, hence, low mobility. For the high oxygen gas-ratio of 0.3, there may be a low density of oxygen vacancies in the oxide film. This may lead to low carrier concentrations and, hence, high mobility. The increased capacitance at a gas flow ratio of 0.3 could be related to the increase of carrier mobility.

To characterise the surface morphology of the lower Co_3O_4 film and the LiPON film, SEM and AFM were employed. The SEM results (not shown) indicate that the surface of the lower Co_3O_4 film (grown at different oxygen gas flow ratios) is very smooth. The AFM studies show that the surface of the LiPON film (grown on the lower Co_3O_4 electrode) is smooth and featureless with a root mean square (rms) roughnesses of 0.75–0.88 nm, as expected from the SEM results. For example, Fig. 5 shows an AFM image of the LiPON film grown at a gas flow ratio of 0.3. The surface is fairly smooth with a rms roughness of 0.75 nm and does not contain channels. The channels connecting the top and bottom sides are known to serve as a leakage source [10]. Compared with the RuO_2 film, as shown in our previous work [10], the Co_3O_4 exhibits fairly smoother morphology.

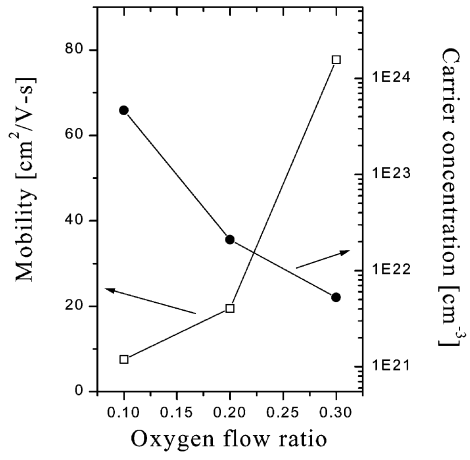

Fig. 4. Carrier mobility and concentration of as-deposited Co_3O_4 films as function of flow ratio. As flow ratio increases, carrier mobility is increased, while carrier concentration is decreased.

In order to investigate the gas-ratio dependence of the microstructures of the Co_3O_4 electrode films, GXRD examination was performed. The GXRD plots for the as-deposited Co_3O_4 film as a function of gas flow ratio [O_2/($Ar + O_2$)] are given in Fig. 6. For the film grown at a flow ratio of 0.1 (Fig. 6(a)) the GXRD plot exhibits characteristic diffraction peaks which are identified to be (2 2 0) Co_3O_4 ($2\theta = 31.9^\circ$), (3 1 1) ($2\theta = 37.1^\circ$), (4 0 0) ($2\theta = 45.2^\circ$), (3 3 3) ($2\theta = 59.18^\circ$), and (4 4 0) ($2\theta = 365.82^\circ$). It is noteworthy that the Co_3O_4 phase has a preferred orientation of (3 1 1). The diffraction peaks are fairly broad, which indicates that the Co_3O_4 film consists of very small grains. For a flow ratio of 0.2 (Fig. 6(b)), the GXRD result is fairly similar to that for a flow ratio of 0.1. For the flow ratio of 0.3 (Fig. 6(c)), however, the (3 1 1) peak intensity is greatly reduced. This indicates that use of the high gas flow ratio leads to the growth of amorphous material. The gas flow ratio dependence of the microstructural characteristics may be related to a change in the sputtering mechanisms due to the increase of the oxygen gas flow ratio [18].With a low oxygen flow ratio ($\leq$0.2), Co atoms (sputtered from the target) can react with oxygen at the substrate surface and form a Co_3O_4 film with the preferred orientation. With a high oxygen flow ratio, a Co-oxide layer may be formed at the target surface. Thus, sputtering of the target (more precisely, Co-oxide) may lead to the formation of amorphous Co_3O_4 materials.

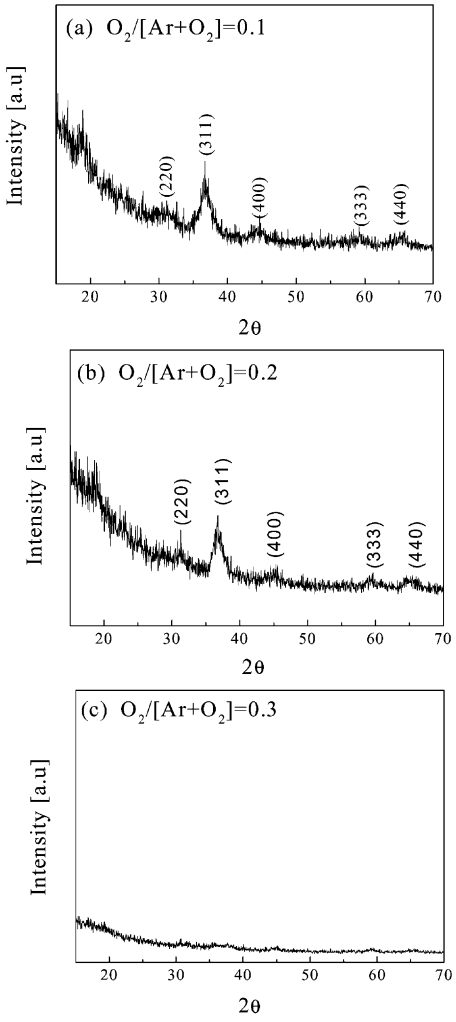

Fig. 6. GXRD plots of Co_3O_4 films grown at oxygen gas-ratios [O_2/($Ar + O_2$)] of: (a) 0.1; (b) 0.2; (c) 0.3.

The charge discharge capacitance of the Co_3O_4/LiPON/Co_3O_4 TFSCs (Fig. 2) may be due to the pseudocapacitance mechanism [6] which is the result of redox processes that involve the reduction of Co_3O_4 to $LiCo_3O_4$, and vice versa. A possible pseudocapacitance mechanism by which the Co_3O_4/LiPON/Co_3O_4 TFSC works is outlined in Fig. 7. During the charge process, Li^+-ions and electrons are incorporated into the lower Co_3O_4 electrode, as shown in Fig. 7(a). During the discharge process, however, the Li^+-ions incorporated into the lower electrode are de-intercalated into the LiPON electrolyte and release electrons (Fig. 7(b)). Following the treatment by Lim et al. [10], the reactions between the Co_3O_4 electrodes and the LiPON electrolyte during cycling could be described by

$$\text{positive electrode}: \quad LiCo_3O_4 + x\text{Li} + x\text{e} \underset{\text{dischage}}{\overset{\text{charge}}{\rightleftarrows}} x\text{LiCo}_3\text{O}_4$$

negative electrode :

$$: x\text{LiCo}_3\text{O}_{4-y} \underset{\text{discharge}}{\overset{\text{charge}}{\rightleftarrows}} \text{Li}_{1-x}\text{Co}_3\text{O}_{4-y} + x\text{Li} + x\text{e}$$

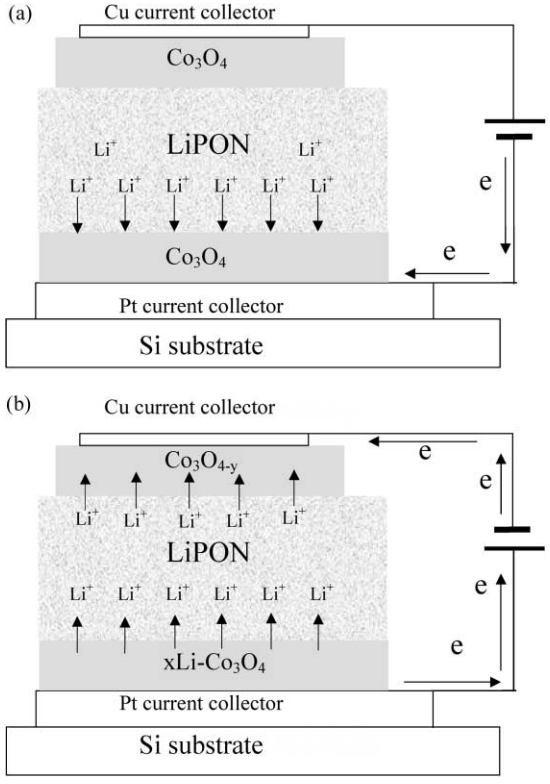

Fig. 7. Possible pseudocapacitance mechanism by which Co_3O_4/LiPON/Co_3O_4 TFSC works: (a) charge state; (b) discharge state.

At the first charging state, the Li-ions are transported to the negative electrode. It is considered that the redox reaction on the Co_3O_4 TFSC involves Li-ion insertion between the positive and the negative electrode, alternately. After the first charge–discharge process, the second charging state follows the above processes.

It is found that the charge discharge capacitance of all the TFSCs fades gradually with increasing cycle number (Fig. 2). In our previous work on TFB [14], the XRD and transmission electron microscopy results showed that the Li^+-intercalation–deintercalation process promoted reactions between V_2O_5 and LiPON which resulted in interfacial products. It was further shown that the cycling process led to a microstructural change of V_2O_5 from an amorphous phase to an amorphous matrix with short-range order and crystallites. Based on the structural results, capacity fade was attributed to the presence of crystallites and interfacial phases [19]. Thus, although no information is available at the moment, the observed degradation of the capacitance in the present samples might be also attributed to structural changes in the Co_3O_4 films.

The above results show that the higher the oxygen gas flow ratio, the better capacitance of the TFSC (Fig. 2). The flow ratio dependence of the capacitance can be explained as follows. First, it can be related to the microstructure of the Co_3O_4 electrode, which changes with the gas flow ratio. The XRD results show that the Co_3O_4 film grown at the high oxygen flow ratio of 0.3 exhibits amorphous characteristics,

while low flow ratios ($\leq$0.2) result in polycrystalline films with very small grains. It is known that the proton-involved reaction of an electrode film is strongly dependent on the structure of the electrode in an electrochemical capacitor which uses an aqueous electrolyte [20]. Thus, considering that an amorphous structure is required to obtain good cycling performance of Li^+-intercalation materials [21], the better capacitance of the TFSC grown at the high gas flow ratio (0.3) can be attributed to the amorphous nature of the Co_3O_4 film. Thus, from the viewpoint of the fabrication of a durable TFSC, the growth of an amorphous Co_3O_4 films is desirable. Another factor can, however, be related to the improved electrical properties. As seen in Fig. 3, the film grown at the high oxygen flow ratio shows better electrical properties than those grown at the two lower flow ratios. Therefore, the dependence of the capacity on the oxygen flow ratio can be attributed to the combined effects of the amorphous structure and the improved electrical properties of the Co_3O_4.

4. Conclusions

All-solid-state TFSCs have been successfully fabricated using Co_3O_4 electrode films, which are grown at different sputtering gas-ratios from 0.1. to 0.3. Room temperature charge–discharge measurements of Co_3O_4/LiPON/Co_3O_4 TFSCs demonstrate that the Co_3O_4-based TFSC exhibits bulk-type supercapacitor behaviour. This indicates that the fabrication of a thin-film type of supercapacitor can be possible with Co_3O_4 electrodes. The capacitance per volume of the Co_3O_4 grown at an oxygen flow ratio of 0.3 is 2.5×10^{-2} F cm^{-2} μm. This value is comparable with that of a RuO_2 TFSC. In addition, it is found that the capacitance behaviour of the Co_3O_4-based TFSC is dependent on the oxygen flow ratio. It is concluded that the different structural and electrical properties of the Co_3O_4 films alter the electrochemical performance of the TFSCs. Possible explanations are given for the flow ratio dependence of the capacitance.

Acknowledgements

This work was supported by the K2000 project and the Brain Korea 21 project.

References

[1] E.J. Jeon, Y.W. Shin, S.C. Nam, W.I. Cho, Y.S. Yoon, J. Electrochem. Soc., in press.
[2] H.-K. Kim, E.J. Joen, Y.-W. Ok, T.-Y. Seong, W.I. Cho, Y.S. Yoon, J. Kor. Inst. Elec. Electron. Mater. Eng. 13 (2000) 751.
[3] E.J. Jeon, Y.S. Yoon, S.C. Nam, W.I. Cho, Y.W. Shin, J. Kor. Electrochem. Soc. 3 (2000) 2 115.
[4] H.-K. Kim, T.Y. Seong, J.H. Lim, W.I. Cho, Y S. Yoon, Kor. J. Mater. Res. 11(5) (2001).
[5] H.-K. Kim, T.-Y. Seong, E.J. Jeon, W.I. Cho, Y.S. Yoon, J. Kor. Ceram. Soc. 38 (2001) 100.
[6] B.E. Conway, Electrochemical Supercapacitors, Plenum, New York, 1999.
[7] H.B. Sierra Alcazar, K.A. Kern, G.E. Mason, R. Tong, in: Proceedings of the 3rd International Power Sources Symposium, Cherry Hill, NJ, 1988, p. 607.
[8] J.P. Zheng, P.J. Cygan, T.R. Jow, J. Electrochem. Soc. 142 (1995) 2699.
[9] J.H. Lim, D.J. Choi, B.H. Son, S.C. Nam, W.I. Cho, Y.S. Yoon, in: Proceedings of the 197th Meeting of the Electrochemical Society, Vol. 44, Toronto, Canada, 2000 (abstract).
[10] J.H. Lim, D.J. Choi, H.-K. Kim, W.I. Cho, Y.S. Yoon, J. Electrochem. Soc. 148 (2001) A278.
[11] Y.S. Yoon, J.H. Lim, D.J. Choi, W.I. Choi, J. Power Source, in press.
[12] R. Singh, J. Koenig, G. Poillerat, P. Chartier, J. Electrochem. Soc. 137 (1990) 1408.
[13] P. Rasiyah, A. Tseung, J. Electrochem. Soc. 130 (1983) 2384.
[14] T.-C. Liu, W.G. Pell, B.E. Conway, Electrochim. Acta 44 (1999) 2829.
[15] B.J. Neudecker, N.J. Dudney, J.B. Bates, J. Electrochem. Soc. 147 (2000) 517.
[16] K. Vanheusden, C.H. Seager, W.L. Warren, D.R. Tallant, J.A. Voigt, Appl. Phys. Lett. 68 (1996) 403.
[17] G.W. Tomlis, J.L. Routbort, T.O. Mason, J. Appl. Phys. 87 (2000) 117.
[18] Y. Kaga, Y. Abe, H. Yanagisawa, K. Sasaki, Jpn. J. Appl. Phys. 37 (1999) 3457.
[19] H.-K. Kim, E.J. Jeon, Y.-W. Ok, T. Y Seong, W.I. Cho, Y.S. Yoon, J. Kor. Ceram. Soc. 38 (2001) 274.
[20] L.M. Da Silva, J.F. Boodts, L.A. DeFaRia, Electrochim. Acta 45 (2000) 2719.
[21] Y. Sakurai, S. Okada, J. Yamaki, J. Power Sources 20 (1987) 173.